

## Beyond Eliashberg Superconductivity in MgB<sub>2</sub>: Anharmonicity, Two-Phonon Scattering, and Multiple Gaps

Amy Y. Liu,<sup>1,2</sup> I. I. Mazin,<sup>2</sup> and Jens Kortus<sup>1,2,3</sup>

<sup>1</sup>*Department of Physics, Georgetown University, Washington, D.C. 20057*

<sup>2</sup>*Center for Computational Materials Science, Code 6390, Naval Research Laboratory, Washington, D.C. 20375*

<sup>3</sup>*MPI für Festkörperforschung, Stuttgart, Germany*

(Received 27 March 2001; published 7 August 2001)

Density-functional calculations of the phonon spectrum and electron-phonon coupling in MgB<sub>2</sub> are presented. The  $E_{2g}$  phonons, which involve in-plane B displacements, couple strongly to the  $p_{x,y}$  electronic bands. The isotropic electron-phonon coupling constant is calculated to be about 0.8. Allowing for different order parameters in different bands, the superconducting  $\lambda$  in the clean limit is calculated to be significantly larger. The  $E_{2g}$  phonons are strongly anharmonic, and the nonlinear contribution to the coupling between the  $E_{2g}$  modes and the  $p_{x,y}$  bands is significant.

DOI: 10.1103/PhysRevLett.87.087005

PACS numbers: 74.25.Kc, 63.20.Ry, 74.25.Jb

The recent discovery of superconductivity near 40 K in MgB<sub>2</sub> has generated much interest in the properties of this simple intermetallic compound [1]. A significant B isotope effect strongly suggests phonon-mediated pairing [2]. To explain the large  $T_c$ , an electron-phonon coupling (EPC) constant of  $\lambda \approx 1$  is needed. Yet estimates of the coupling strength based on the latest measurements of the low-temperature specific heat [3], combined with the density of states (DOS) from density-functional calculations [4], yield  $\lambda \approx 0.6$ – $0.7$ . Further, the measured temperature dependence of the electrical resistivity [5] is consistent with  $\lambda_{tr} \lesssim 0.6$ . First-principles calculations of the EPC give  $\lambda \approx 0.7$ – $0.9$  [4,6,7]. Clearly there is a problem in reconciling all these numbers. Another puzzle involves tunneling measurements of the gap. Values of  $2\Delta/k_B T_c$  ranging from 1.2 to 4 have been reported. The values below the BCS weak-coupling limit of 3.5 have been attributed to surface effects, but the best-quality spectra [8] show a very clean gap with  $2\Delta/k_B T_c = 1.25$ . Sharvin contact measurements [9] reveal a gap at 4.3 meV ( $2\Delta/k_B T_c = 2.6$ ), and additional structures at  $2\Delta/k_B T_c = 1.5$  and 3, raising the possibility of multiple gaps. Careful analysis of the temperature and magnetic-field dependence of the specific heat suggests anisotropic or multiple gap structure as well [3]. Thus, even if superconductivity in MgB<sub>2</sub> is phonon-mediated, it is likely that an analysis beyond the simple isotropic Eliashberg model is needed.

The MgB<sub>2</sub> lattice consists of two parallel systems of flat layers. One layer contains B atoms in a honeycomb lattice, the other Mg atoms in a triangular lattice halfway between the B layers. First-principles calculations [4] find that the electronic states near the Fermi level are primarily B in character and the Fermi surface (FS) comprises four sheets: two nearly cylindrical hole sheets about the  $\Gamma$ - $A$  line arising from quasi-2D  $p_{x,y}$  B bands, and two tubular networks arising from 3D  $p_z$  bonding and antibonding bands [4]. The difference in character between the sheets raises the possibility that each has a distinct gap that could be observed in the clean limit [10]. Such interband

anisotropy enhances the effective EPC constant relevant to superconductivity and decreases the coupling constant for transport, compared to the average values [11–13]. This could explain the discrepant values of  $\lambda$  deduced from different types of experiments.

In this Letter, we report first-principles calculations of the EPC in MgB<sub>2</sub>. The coupling constant is decomposed into contributions from the four different bands crossing the Fermi level, allowing for an analysis of the effects of interband anisotropy on the superconducting  $T_c$  and gap structure. The strongest coupling arises from the  $E_{2g}$  phonon modes along the  $\Gamma$  to  $A$  line, which strongly interact with the quasi-2D electronic states. This phonon mode is calculated to be highly anharmonic, and it also has significant nonlinear contributions to the EPC [14].

Harmonic phonon frequencies and linear EPC parameters were calculated using the linear-response method within the local density approximation (LDA) [15]. Norm-conserving pseudopotentials [16] were used, with a plane-wave cutoff of 50 Ry. We used the experimental crystal structure, with  $a = 3.08$  Å and  $c/a = 1.14$  [17]. The electronic states were sampled on grids of up to  $24^3$   $\mathbf{k}$  points in the full Brillouin zone, and the dynamical matrix was calculated on a grid of  $8^3$  phonon wave vectors  $\mathbf{q}$  [18].

The calculated phonon density of states  $F(\omega)$  and Eliashberg function  $\alpha^2 F(\omega)$  are plotted in Fig. 1. The results are similar to those reported in Refs. [6] and [7]. All of these calculations give a slightly softer phonon spectrum than what is observed in neutron experiments [19]. While  $F$  and  $\alpha^2 F$  are similar in shape in many materials, they are strikingly different in MgB<sub>2</sub>. In particular,  $\alpha^2 F$  has a pronounced peak in the range of 60 to 70 meV arising from dispersive optic modes that do not give rise to large structures in  $F$ . Correspondingly, the average phonon frequency  $\omega_{ave} = 55.3$  meV is less than the logarithmically averaged frequency  $\omega_{ln} = \exp[\lambda^{-1} \int \ln \omega \alpha^2 F(\omega) \omega^{-1} d\omega] = 56.2$  meV, despite the fact that logarithmic averaging preferentially weights

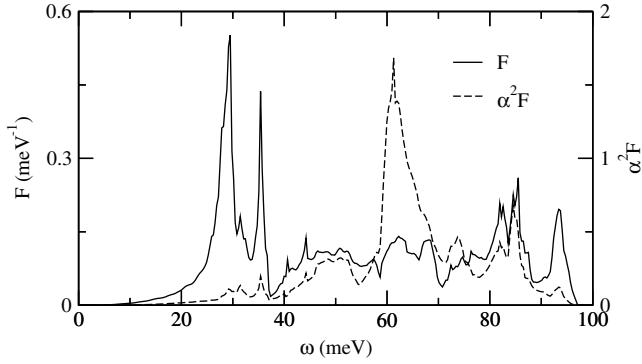


FIG. 1. Phonon density of states and Eliashberg function.

lower frequencies. The isotropic EPC constant, which determines  $T_c$  in the dirty limit,  $\lambda_{sc}^0 = 2 \int \omega^{-1} \alpha^2 F(\omega) d\omega$  is found to be 0.77, in reasonable agreement with other calculations [4,6,7].

The peak in  $\alpha^2 F$  between 60 and 70 meV arises from the  $E_{2g}$  phonon modes with  $\mathbf{q}$  along the  $\Gamma$ -A line. This Raman-active phonon mode, doubly degenerate at  $\Gamma$ , involves in-plane, hexagon-distorting displacements of the B atoms. In fact, by symmetry, this is the only mode at  $\Gamma$  that has a linear EPC. Going away from the  $\Gamma$ -A line the EPC drops sharply when the phonon wave vector  $\mathbf{q}$  becomes larger than the diameter of the 2D Fermi surface; at the same time the frequency increases by roughly 30%. This indicates that the reason why this B-B bond-stretching mode is not the highest-frequency mode at  $\Gamma$  is because of softening due to EPC. However, this softening should weaken in the superconducting state, since some of the screening electrons form Cooper pairs and are removed from the Fermi sea [20]. The overall scale of the relative hardening,  $\Delta\omega/\omega$ , is set by a specific EPC constant,  $\lambda_{ZZ} = 2\omega^{-1} \sum_{\mathbf{k}i} |g_{k,k}|^2 \delta(\epsilon_{\mathbf{k}i})$ , where  $g$  is the EPC matrix element. (The Fermi level is set to zero.) In the BCS limit,  $\Delta\omega/\omega$  is a known analytical function [21] of  $\omega$ . We calculate  $\lambda_{ZZ} = 0.6$ , for the  $E_{2g}$  mode. Taking  $\Delta \sim 5$  meV we predict about a 12% hardening of this mode below  $T_c$ . This shift should be observable in Raman or neutron experiments.

Since the 2D FSs are calculated to play an important role in the EPC, we have decomposed the relevant electronic characteristics in terms of the four sheets of the FS. We list in Table I the partial DOS  $N_j = \sum_{\mathbf{k}} \delta(\epsilon_{\mathbf{k}i})$ , and plasma frequencies  $\omega_{p,i,\alpha\alpha}^2 = \frac{8\pi e^2}{V} W_i = \frac{8\pi e^2}{V} \sum_{\mathbf{k}} v_{\mathbf{k}i,\alpha}^2 \delta(\epsilon_{\mathbf{k}i})$ ,

TABLE I. Band decomposition of the electronic density of states at the Fermi level and in-plane and out-of-plane plasma frequencies. The density of states is in units of states  $\text{Ry}^{-1} \text{spin}^{-1} \text{cell}^{-1}$ , and the plasma frequency is in eV.

	Total	1	2	3	4
$N(E_F)$	4.83	0.66	1.38	1.26	1.52
$\omega_{p,xx}$	7.21	2.91	2.95	3.05	5.04
$\omega_{p,zz}$	6.87	0.44	0.52	4.62	5.06

with  $i = 1(2)$  referring to the light(heavy)-hole 2D sheets of the Fermi surface, and  $i = 3(4)$  to the  $p_z$  bonding (antibonding) sheets. The EPC constant was also decomposed into contributions from scattering of an electron from band  $i$  to band  $j$ :

$$\lambda_{sc}^0 = \sum_{ij} U_{ij} N_i N_j / N = \sum_i \lambda_i N_i / N,$$

$$U_{ij} N_i N_j = 2 \sum_{\mathbf{k}q\nu} \omega_{q\nu}^{-1} |g_{\mathbf{k}i,\mathbf{k}+\mathbf{q}j}^\nu|^2 \delta(\epsilon_{\mathbf{k}i}) \delta(\epsilon_{\mathbf{k}+\mathbf{q}j}).$$

Here  $\omega_{q\nu}$  is the frequency of the corresponding phonon, and  $\lambda_{sc}^0$  is the standard (Eliashberg) isotropic coupling constant. Allowing for interband anisotropy of the order parameter (clean limit), the effective coupling constant for superconductivity  $\lambda_{sc}^{\text{eff}}$  is given by the maximum eigenvalue of the matrix  $\Lambda_{ij} = U_{ij} N_i$ , which is always larger than  $\lambda_{sc}^0$ . Assuming the same interaction parameters  $U_{ij}$  for transport properties, the lowest order variational approximation for the Boltzmann equation corresponds to the transport EPC constant  $\lambda_{tr}^0 = \sum_i \lambda_i W_i / W$ . On the other hand, allowing variational freedom for the different sheets of the Fermi surface yields an effective transport coupling constant which is always smaller than  $\lambda_{tr}^0$ . In effect, the different bands provide parallel channels for conduction, so that when ‘‘scattering-in’’ is neglected,  $W/\lambda_{tr}^{\text{eff}} = \sum_i W_i/\lambda_i$  [13].

The calculated interaction parameters  $U_{ij}$  are listed in Table II. Because of similarities between the two 2D sheets, and between the two 3D sheets, we have simplified the model to allow for two different order parameters for these two sets of bands. This gives  $U_{AA} = 0.47$  Ry,  $U_{BB} = 0.10$  Ry, and  $U_{AB} = 0.08$  Ry, where  $A$  and  $B$  stand for the 2D and 3D bands, respectively. Then  $\lambda_A = 1.19$  and  $\lambda_B = 0.45$ , suggesting de Haas–Alphen mass renormalizations of  $\sim 2.2$  and  $\sim 1.5$ , for the two sets of bands, and specific-heat renormalization of 1.77 [22]. The resulting anisotropic effective coupling constant for superconductivity is  $\lambda_{sc}^{\text{eff}} = 1.01$ . Using the Allen-Dynes approximate formula for  $T_c$  [23], we find that to have  $T_c = 40$  K, a Coulomb pseudopotential of  $\mu^* \approx 0.13$  is needed. This is a more conventional value than the  $\mu^* \approx 0.04$  required when  $\lambda_{sc}^0$  is used. For transport, interband anisotropy reduces the in-plane coupling constant  $\lambda_{x,y}$  from 0.70 to 0.58, but has essentially no effect on the out-of-plane  $\lambda_z = 0.46$  (Table III). This is because the anisotropic formula accounts for the fact

TABLE II. Band decomposition of the electron-phonon interaction.

$ij$	11	12	13	14	22
$U_{ij}$ (Ry)	0.676	0.419	0.064	0.096	0.477
$ij$	23	24	33	34	44
$U_{ij}$ (Ry)	0.064	0.097	0.113	0.106	0.092

TABLE III. Calculated superconducting and transport electron-phonon coupling parameters in both the isotropic limit and with interband anisotropy. The last column contains an average  $\lambda_{\text{tr}}$  appropriate for polycrystalline samples.

	$\lambda_{\text{sc}}$	$\lambda_{\text{tr},x}$	$\lambda_{\text{tr},z}$	$\lambda_{\text{tr,ave}}$
Isotropic	0.77	0.70	0.46	0.60
Multigap	1.01	0.58	0.46	0.54

that the transport is mostly due to the 3D bands in any direction, simply because they couple less with phonons. The measured resistivity [5] can be fit remarkably well with the Bloch-Grüneisen formula using the calculated isotropic  $\alpha_{\text{tr}}^2 F$ , with the in-plane and out-of-plane contributions appropriately averaged for polycrystalline samples [24]. With band anisotropy, the resistivity is slightly underestimated.

The temperature dependence of the individual gaps  $\Delta_i$  in the weak-coupling multigap model is defined by  $\Delta_i = \sum_j U_{ij} N_j \Delta_j \int dE \tanh(\sqrt{E^2 + \Delta_j^2}/2T)/\sqrt{E^2 + \Delta_j^2}$ . As shown in Fig. 2, the larger 2D gap is calculated to be BCS-like, with a slightly enhanced  $2\Delta/T_c$ , while the 3D gap is about 3 times smaller in magnitude. Thus, in the clean limit, MgB<sub>2</sub> should have two very different order parameters, which in turn should affect thermodynamic properties in the superconducting state. Experiments indicate that the coherence length in MgB<sub>2</sub> is close to 50 Å. The mean free path corresponding to the residual resistivity observed in Ref. [5] is more than 1000 Å, so that  $2\pi\xi/l \approx 1/3$ . This is in the reasonably clean regime, and it is likely that the intrinsic resistivity is even smaller. However, stronger defect scattering should be detrimental to superconductivity: using the Allen-Dynes formula with the same  $\mu^* = 0.13$ , we get an isotropic  $T_c = 22$  K. Indeed, irradiation has been found to drastically reduce  $T_c$  [25]. Some of the experimental manifestations of multigap superconductivity would be a reduced and impurity-sensitive specific-heat jump at  $T_c$ , a deviation of the critical-field temperature

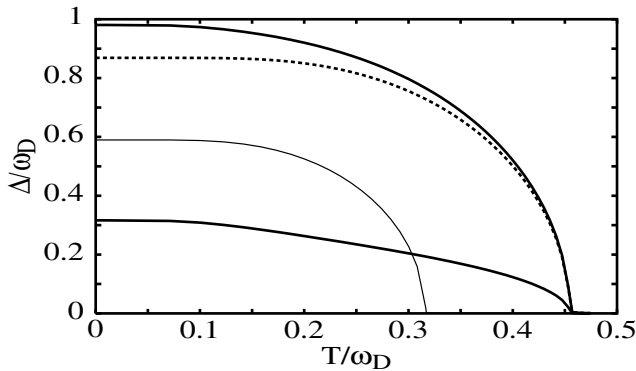


FIG. 2. Ratio of superconducting order parameters  $\Delta_i$  to Debye frequency  $\omega_D$  in the multigap weak-coupling approximation (solid lines), and in the isotropic (dirty) BCS limit (thin line). The BCS order parameter corresponding to the same  $T_c$  as the multigap model is shown by the dashed line.

dependence from the Hohenberg-Werthamer formula, a reduction of the Hebel-Slichter peak in NMR, and a substantial difference between the in-plane and out-of-plane tunneling spectra. In particular, the latter should see only the smaller gap [26].

Note that  $\lambda \sim 1$  is in the intermediate-coupling regime. Furthermore, the multigap scenario suggests particular sensitivity to impurity scattering. This means one should really solve the anisotropic Eliashberg equations with impurity scattering, rather than the weak-coupling BCS equations we used. Thus we do not make any quantitative thermodynamic and spectroscopic predictions here.

We focus now on the  $E_{2g}$  phonon modes, which contribute strongly to the EPC. We have examined this mode at  $\Gamma$  in detail with frozen-phonon calculations using a general-potential linearized augmented plane wave code as in Ref. [4]. This mode has substantial anharmonicity. A fit of the total energy for B displacements  $u$  between  $\pm 0.1$  a.u. to a fourth-order polynomial ( $E_{\text{tot}} = \sum a_n u^n$ ) gives  $a_2 = 0.42$  Ry/a.u.<sup>2</sup>,  $a_3 = -0.66$  Ry/a.u.<sup>3</sup>, and  $a_4 = 3.73$  Ry/a.u.<sup>4</sup> for displacements parallel to one set of B-B bonds. For the other  $E_{2g}$  displacement pattern (i.e., perpendicular to B-B bonds), we obtain the same values for  $a_2$  and  $a_4$ , but  $a_3 = 0$  by symmetry. Anharmonicity increases the  $E_{2g}$  frequency by about 15%, which should result in an overall reduction of  $\lambda$  by  $\sim 10\%$ , and an increase of  $\omega_{\text{lin}}$  by  $\sim 6\%$ .

More interestingly, the  $E_{2g}$  modes have a significant nonlinear coupling with electrons. The linear coupling vertex,  $g_1$ , corresponding to scattering by a single phonon, is proportional to matrix elements of  $dV/dQ$ , where  $Q = \sqrt{2M\omega} u$ , while the second-order coupling, involving exchange of two phonons, is proportional to matrix elements of  $d^2V/dQ^2$ . At  $\Gamma$ , the Hellman-Feynman theorem allows the calculation of  $g_1$  via deformation potentials. This is no longer the case for  $g_2$ . One can use  $d^2\epsilon_{\mathbf{k}}/dQ^2$  only as a qualitative estimate of  $\langle d^2V/dQ^2 \rangle$ . For the cylindrical sheets of the Fermi surface, with B displacements parallel to bonds,  $\langle (d^2\epsilon_{\mathbf{k}}/dQ^2)^2 \rangle^{1/2} = 72$  and 40 mRy as compared to  $\langle (d\epsilon_{\mathbf{k}}/dQ)^2 \rangle^{1/2} = 20$  and 20 mRy. This suggests that nonlinear pairing via *two-phonon* exchange is comparable to or even larger than the linear coupling. The reason for this anomalous behavior lies in the specifics of the band structure of the 2D  $p_{x,y}$  bands. In the nearest-neighbor tight-binding approximation it can be described as

$$\begin{aligned} \epsilon_{\mathbf{k}}^2 &= u_{\mathbf{k}} \pm v_{\mathbf{k}}, \\ 4u_{\mathbf{k}} &= (t_{\pi}^2 + t_{\sigma}^2) \left( 6 + \sum_i \cos G_i \right) + 6t_{\pi} t_{\sigma} \sum_i \cos G_i, \\ (4v_{\mathbf{k}})^2 &= 4(t_{\pi}^2 - t_{\sigma}^2)^2 \left( \sum_i \cos^2 G_i - \sum_{i \neq j} \cos G_i \cos G_j \right) \\ &\quad + 3(t_{\pi} - t_{\sigma})^4 \left( \sum_i \sin G_i \right)^2, \end{aligned}$$

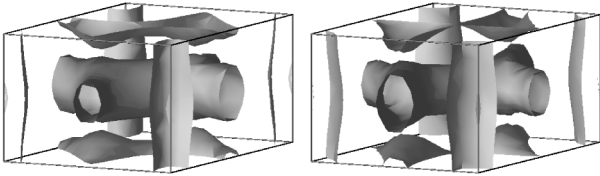


FIG. 3. Fermi surfaces for two frozen-phonon patterns of  $E_{2g}$  symmetry with B displacements of  $\pm 0.07$  a.u.

where  $G_i = \mathbf{a}_i \cdot \mathbf{k}$ , and  $\mathbf{a}_i$  are the three smallest lattice vectors. At the  $\Gamma$  point  $v_{\mathbf{k}} = 0$ , and there are two doubly degenerate states. The bonding pair forms the 2D Fermi surfaces, and the main effect of the  $E_{2g}$  phonons is to lift the degeneracy at  $\Gamma$ , thereby changing the overall splitting between the two subbands. This effect does not depend on the sign of the ionic displacement (the degeneracy is lifted either way) and thus is nonlinear by definition. This is illustrated in Fig. 3 by the Fermi-surface plots for two opposite  $E_{2g}$  phonon patterns, both corresponding to  $Q \approx 1$ . One can see that while for the 3D sheets the coupling is mostly linear (changes of the Fermi surface are opposite), for the 2D cylinders it is mostly quadratic (changes are the same; cf. the undistorted Fermi surface in Ref. [4]). Nonlinear EPC is also a likely source of anharmonicity: as discussed above, the contribution to the  $E_{2g}$  phonon self-energy from the EPC with the 2D FSs amounts to as much as 20 meV, as evidenced by the softening of this phonon at  $\Gamma$ . A sizable part of this softening probably comes from two-phonon processes. Quartic anharmonicity of the ion-ion interaction arises in the fourth order in the linear interaction constant, but in the second order in the nonlinear one.

In summary, we have presented a first-principles investigation of the electron-phonon coupling in  $\text{MgB}_2$ . Interband anisotropy enhances the coupling constant from its isotropic dirty-limit value of  $\lambda_{\text{sc}}^0 = 0.77$  to an effective clean-limit value of  $\lambda_{\text{sc}}^{\text{eff}} = 1.01$  for superconductivity. With  $\omega_{\text{in}} = 56.2$  meV, this  $\lambda_{\text{sc}}^{\text{eff}}$  is arguably consistent with the measured  $T_c$  of nearly 40 K. In the clean limit, we predict two different superconducting order parameters: a larger one on the 2D FSs and a smaller one (by approximately one-third) on the 3D FSs. Since current experiments suggest that  $\text{MgB}_2$  is indeed in the clean limit, multiple gaps should be observable. There are hints of this in both the tunneling and thermodynamic data.

The  $E_{2g}$  phonon mode involving in-plane B motion provides the strongest coupling. We predict a hardening of  $\sim 12\%$  of this mode at the zone center below  $T_c$ . In addition, this mode is highly anharmonic, and it may also have significant two-phonon coupling. The former likely reduces the linear EPC, while the latter increases the total EPC. Both effects may contribute to the significant deviation of the total isotope coefficient from 0.5. Further work

is needed to better elucidate the effect of anharmonicity and nonlinear coupling on the superconducting properties of this material.

We thank J.K. Freericks for helpful discussions. This work was supported by NSF under Grant No. DMR-9973225 and by ONR. A.Y.L. acknowledges support from the ASEE-U.S. Navy Faculty Sabbatical Program.

- [1] J. Nagamatsu *et al.*, Nature (London) **410**, 63 (2001).
- [2] S. L. Bud'ko *et al.*, Phys. Rev. Lett. **86**, 1877 (2001).
- [3] Y. Wang *et al.*, Physica (Amsterdam) **355C**, 179 (2001); F. Bouquet *et al.*, Phys. Rev. Lett. **87**, 047001 (2001).
- [4] J. Kortus *et al.*, Phys. Rev. Lett. **86**, 4656 (2001).
- [5] P. Canfield *et al.*, Phys. Rev. Lett. **86**, 2423 (2001).
- [6] Y. Kong *et al.*, Phys. Rev. B **64**, 020501 (2001).
- [7] K.-P. Bohnen, R. Heid, and B. Renker, Phys. Rev. Lett. **86**, 5771 (2001).
- [8] G. Rubio-Bollinger, H. Suderow, and S. Vieira, Phys. Rev. Lett. **86**, 5582 (2001).
- [9] H. Schmidt *et al.*, Phys. Rev. B **63**, 220504 (2001).
- [10] S. V. Shulga *et al.*, cond-mat/0103154.
- [11] H. Suhl, B. T. Matthias, and L. R. Walker, Phys. Rev. Lett. **3**, 552 (1959).
- [12] W. H. Butler and P. B. Allen, in *Superconductivity in d- and f-band Metals*, edited by D. H. Douglass (Plenum, New York, 1976).
- [13] I. I. Mazin *et al.*, Physica (Amsterdam) **209C**, 125 (1993).
- [14] T. Yildirim *et al.*, cond-mat/0103469.
- [15] A. A. Quong and B. M. Klein, Phys. Rev. B **46**, 10734 (1992); A. Y. Liu and A. A. Quong, *ibid.* **53**, 7575 (1996).
- [16] N. Troullier and J. L. Martins, Phys. Rev. B **43**, 8861 (1991).
- [17] E. L. Muetterties, *The Chemistry of Boron and Its Compounds* (Wiley, New York, 1967).
- [18] Neglecting interband scattering, it is not possible for an optic mode at  $\mathbf{q} = 0$  to couple to electrons since energy cannot be conserved. The contribution to the EPC from the region near  $\Gamma$  is estimated by assuming a constant matrix element in this region and approximating the Fermi surface as two cylindrical sheets [21].
- [19] R. Osborn *et al.*, Phys. Rev. Lett. **87**, 017005 (2001).
- [20] R. Zeyher and G. Zwicknagl, Solid State Commun. **66**, 617 (1988); Z. Phys. B **78**, 175 (1990).
- [21] C. O. Rodriguez *et al.*, Phys. Rev. B **42**, 2692 (1990).
- [22] Current experiments [3] indicate renormalization of 1.6, but the LDA may overestimate the DOS by 10%–15%. The overestimation of NMR relaxation rates by the LDA provides indirect evidence of this [E. Pavarini (unpublished)].
- [23] P. B. Allen and R. C. Dynes, Phys. Rev. B **12**, 905 (1975).
- [24] D. Stroud, Phys. Rev. B **12**, 3368 (1975).
- [25] A. E. Karkin *et al.*, cond-mat/0103344.
- [26] In Ref. [8], where high-quality spectra with a gap 3 times smaller than the BCS value were obtained, a unique procedure was used for sample preparation, which may have preferentially oriented individual microcrystals.